CORRECTION

Correction: Ontogenetic changes in limb posture, kinematics, forces and joint moments in American alligators (*Alligator mississippiensis*)

Masaya Iijima, V. David Munteanu, Ruth M. Elsey and Richard W. Blob

There was an error in *J. Exp. Biol.* (2021) **224**, jeb242990 (doi:10.1242/jeb.242990).

In the Materials and Methods, the term 'SHL' was incorrectly defined in the text of the following sentence:

'The CoM was represented as a percentage of the shoulder–hip distance (CoM$_{SH}$), using an equation: CoM$_{SH}$=100[W_2×L/(W_1+W_2)−SSL]/(SHL−SSL), where L is the length of the beam, SHL is the shoulder–hip length, SSL is the snout–shoulder length, and W_1 and W_2 are the masses recorded at the cranial and caudal balances, respectively.'

The definition of SHL should be 'snout–hip length'. In all their analyses, the authors calculated the CoM using the correct values for snout–hip length.

Both the online full-text and PDF versions of the article have been updated. The authors apologise to readers for this error and any confusion it may have caused.

RESEARCH ARTICLE

Ontogenetic changes in limb posture, kinematics, forces and joint moments in American alligators (*Alligator mississippiensis*)

Masaya Iijima[1,2,*], V. David Munteanu[1], Ruth M. Elsey[3] and Richard W. Blob[1,*]

ABSTRACT

As animals increase in size, common patterns of morphological and physiological scaling may require them to perform behaviors such as locomotion while experiencing a reduced capacity to generate muscle force and an increased risk of tissue failure. Large mammals are known to manage increased mechanical demands by using more upright limb posture. However, the presence of such size-dependent changes in limb posture has rarely been tested in animals that use non-parasagittal limb kinematics. Here, we used juvenile to subadult American alligators (total length 0.46–1.27 m, body mass 0.3–5.6 kg) and examined their limb kinematics, forces, joint moments and center of mass (CoM) to test for ontogenetic shifts in posture and limb mechanics. Larger alligators typically walked with a more adducted humerus and femur and a more extended knee. Normalized peak joint moments reflected these postural patterns, with shoulder and hip moments imposed by the ground reaction force showing relatively greater magnitudes in the smallest individuals. Thus, as larger alligators use more upright posture, they incur relatively smaller joint moments than smaller alligators, which could reduce the forces that the shoulder and hip adductors of larger alligators must generate. The CoM shifted nonlinearly from juveniles through subadults. The more anteriorly positioned CoM in small alligators, together with their compliant hindlimbs, contributes to their higher forelimb and lower hindlimb normalized peak vertical forces in comparison to larger alligators. Future studies of alligators that approach maximal adult sizes could give further insight into how animals with non-parasagittal limb posture modulate locomotor patterns as they increase in mass and experience changes in the CoM.

KEY WORDS: Locomotion, Biomechanics, Ground reaction force, Center of mass, Archosaur

INTRODUCTION

Body size is one of the most important traits that influences the terrestrial locomotor capacities of tetrapods. Although larger animals can take advantage of the reduced weight-specific cost of locomotion (Heglund and Taylor, 1988; Kram and Taylor, 1990; Reilly et al., 2007), they must also accommodate mechanical limitations of the musculoskeletal system. If the shapes and properties of anatomical structures were geometrically similar among animals of different sizes, then larger ones would have to cope with reduced force-generating capacity of their muscles, and an increased risk of tissue failure (Biewener and Patek, 2018). This is because the demands placed on muscle and bone typically increase in proportion to body mass, or L^3, but muscle force generation and the peak stresses that muscle, tendon and bone can accommodate would scale in proportion to their cross-sectional areas, or L^2 (Biewener and Patek, 2018; McMahon, 1973, 1975a). Animals use multiple strategies to deal with such size-dependent increases in mechanical demands, with the strategies that a species uses appearing to relate to whether it employs parasagittal or non-parasagittal limb kinematics (Biewener, 1983; Cieri et al., 2021).

Mammals that use parasagittal locomotion show a tendency to change limb posture with increasing body mass: smaller species of mammals use more crouched limb posture, whereas larger species use more erect posture (Biewener, 1983; Gray, 1968; Gregory, 1912). Because the vector of the ground reaction force (GRF) aligns more closely with erect limb bones, the effective mechanical advantage (EMA) of limb muscles (i.e. the ratio of the muscle moment arm to the GRF moment arm) is greater in large, upright mammals (Biewener, 1983, 1989, 1990, 2005, 2015). Together with generally positive scaling of muscle and bone cross-sectional areas versus body mass (Alexander et al., 1979a, 1981; Bertram and Biewener, 1990; Campione and Evans, 2012; McMahon, 1975b; Pollock and Shadwick, 1994), positive EMA scaling ($\propto$mass$^{0.25}$; Biewener, 1989, 2005) contributes to maintaining similar magnitudes of bone and muscle stresses across wide size ranges of mammals (Biewener, 1990, 2005). Birds show similar size-dependent trends for limb posture (more upright hindlimbs in larger species), which also result in the increased EMA of hindlimb muscles (Daley and Birn-Jeffery, 2018; Gatesy and Biewener, 1991).

Among tetrapods that use non-parasagittal limb posture, varanid and iguanid lizards show positive scaling of limb muscle and bone cross-sectional areas (Blob, 2000; Christian and Garland, 1996; Cieri et al., 2020; Dick and Clemente, 2017), but limb posture during running seems to be similar across species that span a wide range of body masses (Clemente et al., 2011). Although duty factor increases and locomotor speed decreases among larger varanids (Cieri et al., 2021; Clemente et al., 2012), it remains uncertain whether their muscle and bone stresses are maintained at similar magnitudes. Bone stress estimations based on GRFs and muscle forces in green iguanas suggested that femoral bending stresses would be higher when using more upright limb posture (Blob and Biewener, 2001), which might explain why larger lizards do not use more upright stance.

Crocodylians are large quadrupeds that use diverse limb postures from a belly walk to a high walk, although the belly walk is primarily used for a transition to and from high walk posture (Brinkman, 1980; Gatesy, 1991; Reilly and Elias, 1998). Ancestrally, early pseudosuchians (crocodylian-line archosaurs

[1]Department of Biological Sciences, Clemson University, Clemson, SC 29634, USA. [2]Nagoya University Museum, Furocho, Chikusa-Ku, Nagoya, Aichi 464-8601, Japan. [3]Louisiana Department of Wildlife and Fisheries, Rockefeller Wildlife Refuge, 5476 Grand Chenier Highway, Grand Chenier, LA 70643, USA.

*Authors for correspondence (miijima8@gmail.com; rblob@clemson.edu)

M.I., 0000-0003-2701-0391; R.W.B., 0000-0001-5026-343X

that first appeared in the Early Triassic; Nesbitt, 2011) showed morphological adaptations suited for parasagittal limb posture, including downward facing acetabula (Benton and Clark, 1988; Bonaparte, 1984; Parrish, 1986, 1987). Because of a likely secondary acquisition of non-parasagittal limb posture among modern crocodylians, limb kinematics (e.g. femur and knee angles and movements during stance) of the high walk are intermediate between kinematics of parasagittal and sprawling posture in the postural continuum (Charig, 1972; Gatesy, 1991; Nyakatura et al., 2019; Reilly and Elias, 1998). Therefore, studies of size-dependent changes in limb geometries and locomotion in crocodylians can provide a distinct insight into the strategies used to address increasing mechanical demands with larger body size among animals that use postures intermediate between strictly sprawling and parasagittal.

Previous intraspecific and interspecific comparisons of limb muscles and bones in crocodylians showed an overall geometric similarity of limb muscle cross-sectional areas and positive allometry of limb bone diameters and circumferences versus lengths, the latter of which might help maintain similar bone stresses across a range of body sizes (Allen et al., 2010; Blob, 2000; Iijima and Kubo, 2019). Meanwhile, bending stresses of the femur increase with more upright posture in juvenile alligators, which might be explained by greater activation of knee extensor muscles that compress the dorsal cortex of the femur during upright stance (Blob and Biewener, 1999; Reilly and Blob, 2003). However, it remains unknown whether small and large alligators use similar limb postures, as found for interspecific comparisons of monitor lizards (Clemente et al., 2011).

In this study, we measured forelimb and hindlimb kinematics and kinetics across American alligators ranging from small juveniles to subadults (body mass 0.3–5.6 kg). By integrating measurements of limb kinematics with speed and stride parameters, GRFs, joint moments and center of mass (CoM), we tested for ontogenetic shifts in posture and limb mechanics in alligators to evaluate the generality of patterns among non-parasagittal tetrapods. If alligators use a similar posture throughout ontogeny, it could lend support to the hypothesis that differences in limb anatomy between mammals and non-avian sauropsids (e.g. alligators and iguanas) lead to differences in how hindlimb muscles and bone loading are modulated over the limb posture gradient: the use of more upright posture does not help non-avian sauropsids to reduce bone stresses (Reilly and Blob, 2003). Conversely, if larger alligators use more upright posture as shown in the interspecific comparisons of mammals, the reason as to why they choose a posture that could increase bone stresses would require explanation.

MATERIALS AND METHODS
Animals
Twelve juvenile to subadult American alligators, *Alligator mississippiensis* (Daudin 1802), were provided by the Rockefeller Wildlife Refuge, Grand Chenier, LA, USA. These animals were hatched in the wild and collected by Louisiana Department of Wildlife and Fisheries alligator program staff biologists and technicians. Animals used for walking trials were divided into three size classes: small (*n*=3, total length 0.46–0.48 m, body mass 0.23–0.26 kg), medium (*n*=3, total length 0.81–0.90 m, body mass 1.40–2.06 kg) and large (*n*=1, total length 1.27 m, body mass 5.64 kg). Sexes and ages of animals were unknown. The sampled range of body mass is narrower than that in the previous interspecific comparison of crocodylian locomotion (Hutchinson et al., 2019). However, the large individuals approach the maximum

size that we could keep in our animal facility. Animals were individually housed at Clemson University in enclosures filled with shallow water in a greenhouse vivarium facility, with ambient lighting and humidity, daytime temperatures between 23 and 38°C, and periodically open roof panels to provide natural sunlight and UV. Small and medium individuals were fed commercial pellets for crocodylians (Mazuri crocodilian diet, small), and large individuals were offered pellets, live feeder fish, or pieces of boneless chicken or pork twice a week. Animal care and experimental procedures were approved by Clemson University IACUC (protocol 2019-037). Measurements of just CoM were obtained from 33 additional individuals (total length 0.47–1.55 m, body mass 0.25–8.00 kg) housed at Clemson University and the Rockefeller Wildlife Refuge.

### Data collection and processing
Walking trials were conducted on a wooden trackway fitted with a force plate that was made level with the walking surface, and with a clear panel on one side to facilitate video imaging. Room temperature was controlled at 23°C, and animals were allowed to rest under heat lamps for several minutes between the trials. Animals were filmed simultaneously from lateral and dorsolateral views with two digitally synchronized Phantom v.5.1 high-speed cameras (Vision Research, Wayne, NJ, USA) at 100 Hz. Single-foot GRFs of the forelimb and hindlimb were recorded at 5000 Hz from either a custom-built K&N Scientific (Guilford, VT, USA) force plate (see Butcher and Blob, 2008 for specifications) or a Kistler (Novi, MI, USA) force plate (type 9260AA3Y0500), using custom LabVIEW routines (v.6.1, National Instruments, Austin, TX, USA). Plate calibrations were conducted manually (K&N Scientific plate) or from verified manufacturer specifications (Kistler plate) each day of trials. Force data were synchronized with video using a trigger that simultaneously sent a 1.5 V square-wave pulse to a force trace channel and a light pulse to video. Raw force signals were processed by averaging values to produce samples at 50 Hz. Force baselines were corrected to zero using data 0.02 s before foot touchdown, as indicated by video frames. Force data and kinematics were analyzed only for the stance phase duration of a footfall.

To obtain 3D coordinates of the anatomical landmarks for kinematic measurements, white dots of correction fluid were painted on the right forelimb (metacarpophalangeal joint of digit III, wrist, elbow and shoulder joints), right hindlimb (metatarsophalangeal joint of digit III, ankle, knee and hip joints) and midline of the trunk (medial to the right shoulder and hip, and three equidistant points between them). The 3D space through which animals walked was calibrated via DLTcal5 software using toy building bricks of known dimensions, with 3D coordinates of landmarks digitized using DLTdv7 (Hedrick, 2008) in MATLAB R2019b. Frames during stance (touchdown to toe-off) of each limb were digitized at various rates depending on the stance duration. Walking speed during a single stride was measured by tracking the landmarks on the midline of the body. Speed during an entire stride, rather than just stance phase, was measured to evaluate steady speed over a longer duration. Only steady speed and straight walks with the placement of a whole foot on the force plate were chosen for analyses. Steady speed was evaluated by ordinary least squares regressions of the instantaneous velocities (0.1 s intervals) over a single stride versus the time elapsed (Granatosky, 2016). Trials that involved significant acceleration or deceleration (α=0.01) were excluded. Kinematic and force data were synchronized by resampling 5% increments of data points during stance, with variables at 21 evenly spaced time points interpolated using the function approxfun() in R (https://www.r-project.org/).

Joint coordinate systems for the forelimb and hindlimb followed Sullivan (2007). Three rotational degrees of freedom were considered for the shoulder and hip, whereas only flexion–extension was considered for elbow, wrist, knee and ankle joints, owing to limitations of skin marker-based measurements of limb kinematics. For the shoulder and hip in the reference pose (forelimb and hindlimb fully extended and pointing laterally; Fig. 1A–C), the x-axis (pink) points laterally, coincides with the long axis of the humerus and femur, and with rotation about this axis representing their external–internal rotation. The y-axis (green) points posteriorly, perpendicular to the x- and z-axes, with rotation about this axis representing abduction–adduction. The z-axis (blue) points ventrally, perpendicular to the x- and y-axes and in the same plane as the shoulder, elbow and wrist in the forelimb and the hip, knee and ankle in the hindlimb (Blob and Biewener, 2001), with rotation about this axis representing retraction–protraction. Joint angles from the reference pose were measured for each of the three rotational axes of the shoulder and hip. The rotation order of the three axes was z-y-x, and the right-hand rule convention (counterclockwise positive and clockwise negative rotation as viewed from the arrow tip) was used. Long axis rotation was measured using the shoulder, elbow and wrist landmarks for the humerus in the forelimb, and the hip, knee and ankle landmarks for the femur in the hindlimb, assuming that elbow and knee abduction–adduction is minimal during stance (Clemente et al.,

2011; Irschick and Jayne, 2000). We acknowledge that the skin marker-based flexion–extension axes of the elbow, wrist, knee and ankle could change with respect to osteologically defined joint axes during stance owing to abduction–adduction, long axis rotation and translation about the joints (Manafzadeh and Gatesy, 2021; Manafzadeh et al., 2021; Sullivan, 2007); thus, the method we employed should be regarded as providing only approximate kinematic measurements.

Joint moments exerted by the GRF were calculated for each of the rotational axes in the forelimb and hindlimb, based on the GRF vectors and the joint coordinates. The GRF vector was resolved into the directions of two axes perpendicular to each other and to the rotational axis of interest, and then two opposing moments about the rotational axis were summed (Fig. 1D). For example, to calculate the hip abduction–adduction moment, the GRF vector was first resolved into two components parallel to the long axis of the femur (GRF_x) and the hip retraction–protraction axis (GRF_z). Given that moment arms of GRF_x and GRF_z about the rotational axis are R_z and R_x, respectively, the hip abduction–adduction moment is $R_x \times GRF_z - R_z \times GRF_x$ (Fig. 1D). The right-hand rule convention for a positive moment about each rotational axis was used. Because forelimb and hindlimb steps sometimes had minor overlap during either the ending of steps for the forelimb or the beginning of stance for the hindlimb, the center of pressure (CoP) of each step was estimated from video. At the beginning of stance, the CoPs were
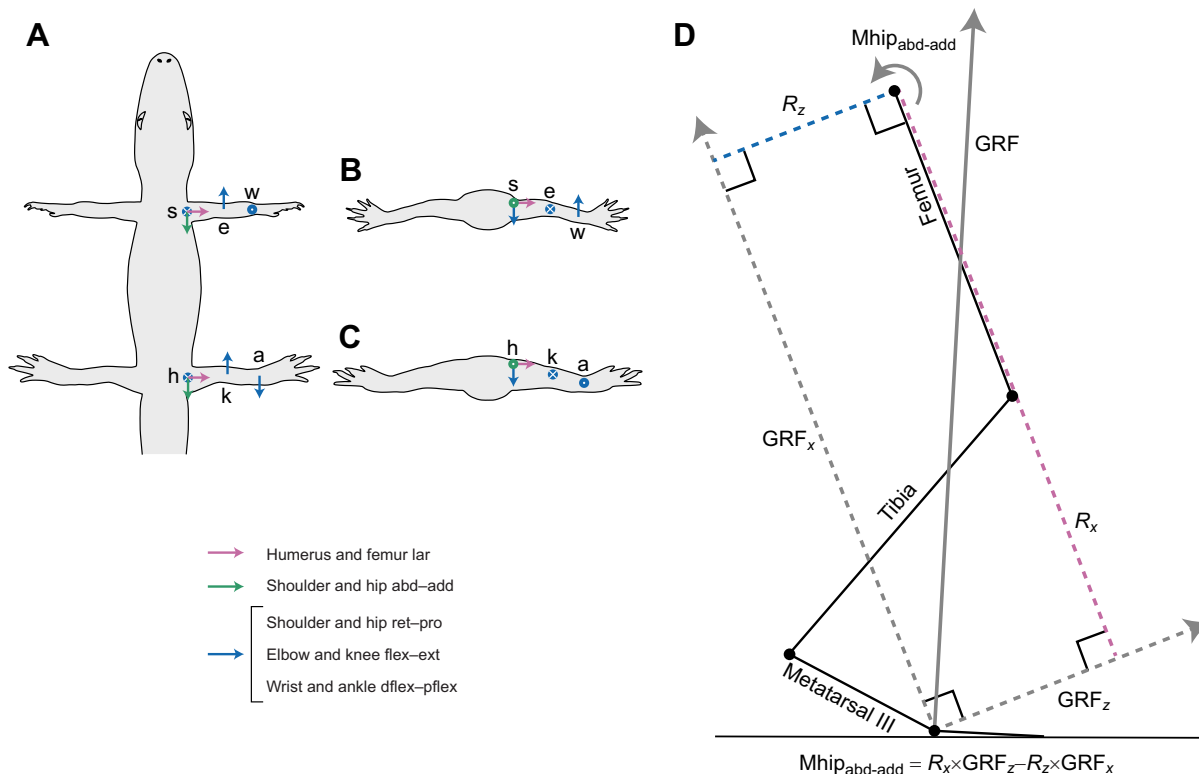
Fig. 1. The reference pose and joint coordinate systems for the forelimb and hindlimb and an example of the joint moment calculation. (A) Dorsal view of the body, and (B,C) posterior views of the forelimb and hindlimb, respectively. x- (pink), y- (green) and z- (blue) rotational axes represent long axis rotation, abduction–adduction, and retraction–protraction (for shoulder and hip) or flexion–extension (for distal joints), respectively. Right-hand rule convention (counterclockwise positive and clockwise negative rotation as viewed from the arrowhead) was used. The circled dot and circled × indicate the arrowhead and the opposite end, respectively. (D) Calculation of the hip abduction–adduction moment (Mhip$_{abd-add}$). The ground reaction force (GRF) was resolved into two components parallel to the long axis of the femur (GRF_x) and the hip retraction–protraction axis (GRF_z). Given that the moment arms of GRF_x and GRF_z about the rotational axis are R_z and R_x, respectively, Mhip$_{abd-add}$ was calculated as $R_x \times GRF_z - R_z \times GRF_x$. Joint abbreviations: a, ankle; e, elbow; h, hip; k, knee; s, shoulder; w, wrist. Limb movement abbreviations: abd, abduction; add, adduction; dflex, dorsiflexion; ext, extension; flex, flexion; lar, long axis rotation; pflex, plantarflexion; pro, protraction; ret, retraction.

positioned at the metacarpophalangeal and metatarsophalangeal joint landmarks, respectively, because those joints are approximately in the center of the foot contact surfaces. As the forefoot and hindfoot start to lift off the ground, the CoPs were constantly moved towards the tip of the digit III until toe-off (Blob and Biewener, 2001). Joint moments calculated here should be interpreted with caution, because skin markers were displaced from osteological joint centers and would incur some error. We did not measure joint moments from segment inertia and gravity, which might cause some error in calculations of total joint moment, particularly at proximal joints.

The horizontal CoM of each alligator was measured using two balances (Clemente, 2014). A wooden or Plexiglas beam was loaded on two balances, where each end of the beam was supported at the center of each balance. The animals were placed on the beam in a neutral posture (elbow and knee pointing laterally and forearm and lower leg parallel to the body axis), with the snout tip aligned with the end of the beam, and maintained a steady position during measurement. The CoM was represented as a percentage of the shoulder–hip distance (CoM_{SH}), using the following equation: $\text{CoM}_{\text{SH}}=100[W_2 \times L/(W_1+W_2)-\text{SSL}]/(\text{SHL}-\text{SSL})$, where L is the length of the beam, SHL is the snout–hip length, SSL is the snout–shoulder length, and W_1 and W_2 are the masses recorded at the cranial and caudal balances, respectively. A CoM_{SH} of 0 or 100 would indicate the CoM positioned at the shoulder or hip, respectively.

Data visualization and statistical analyses

A bivariate plot showing the relationship of the limb phase (ratio of the duration between the touchdown of a forelimb and its ipsilateral hindlimb to the total stride time; modified from Hildebrand, 1976) and duty factor was made to compare gaits among the three size classes of alligators. Only trials where steady-speed forelimb and hindlimb steps were filmed in a single video were used for gait comparisons. Speed and stride parameters, joint angles, normalized peak forces and normalized peak joint moments were compared for the forelimb and hindlimb among the three size classes. Speed and stride parameters included: (1) dimensionless speed [$u(\bm{g} \cdot h)^{-0.5}$], where u is walking speed, $\bm{g}$ is the acceleration of gravity and h is the extended hip to ankle length; (2) stride duration; (3) duty factor; and (4) stride length standardized to the total length. The joint angles compared for each limb were: (1) retraction–protraction, (2) adduction, (3) long axis rotation angles of the humerus and femur, (4) flexion angles of the elbow and knee, and (5) plantarflexion angles of the wrist and ankle. Angles 1 and 3 were compared as excursions (maximum minus minimum angles) and angles 2, 4 and 5 were compared as mean angles during mid-stance (25–75% of stance). Force parameters compared were: (1) peak vertical forces, (2) peak propulsive forces, (3) peak braking forces, (4) peak medial forces normalized to body weight unit and (5) average GRF medial inclination angles (angles between GRF vectors and the plane including the dorsoventral axis and the direction of travel) during mid-stance. Normalized peak joint moments (N·m kg$^{-4/3}$) compared were: (1) shoulder and hip protraction and retraction moments, (2) shoulder and hip abduction moments, (3) humerus and femur external and internal rotation moments, (4) elbow and knee flexion moments, and (5) wrist and ankle dorsiflexion moments. Joint moments (N·m) were normalized by the 4/3 power of body mass (kg$^{4/3}$) following the convention of human biomechanical studies that use body mass (kg) times a linear dimension (m) such as body height as a normalization factor (Moisio et al.,

2003), which scales with kg$^{4/3}$ under the assumption of isometric growth.

Linear mixed effects models were employed to compare the speed, stride, joint angle, force and peak joint moment variables among the three size classes of alligators, with the size class and dimensionless speed as fixed effects, intercept for individuals as a random effect, and no interaction term, using the package lme4 (Bates et al., 2015) in R v.3.6.3 (https://www.r-project.org/). For the comparison of dimensionless speed, only the size class was used as a fixed effect. ANOVA comparing the full model and the reduced model without the size class as a fixed effect was conducted to test for a significant effect of size class (α=0.05) and the effect size Ω^2 (Xu, 2003) was calculated using the R package performance (Lüdecke et al., 2020). Additionally, *post hoc* pairwise comparisons of all size class pairs were performed using the R package multcomp (α=0.05) (Hothorn et al., 2008). Comparisons were visually aided by line plots of joint angles, GRFs and joint moments. To evaluate degrees of overall forelimb and hindlimb flexion, shoulder and hip height profiles during stance were also calculated. Walking trials where the shoulder and hip heights at touchdown and toe-off differed by more than 10% were excluded. Line plots were created using 5% increments of data points during stance.

RESULTS

Seven alligators from three size classes (three small, three medium and one large) performed steady speed walks, and 73 forelimb strides (32, 25 and 16 strides for small, medium and large size classes, respectively) and 63 hindlimb strides (22, 21 and 20 strides for small, medium and large size classes, respectively) were recorded (Movies 1–3). Alligators chose gaits that included walking trots and diagonal couplet walks (Hildebrand, 1976) irrespective of size class, with limb phases of 0.43–0.59 (Fig. S1). No aerial phase was observed in any trial.

Dimensionless speed was faster in the smaller size classes, and stride duration was longer in the large size class than the small and medium size classes for the forelimb and hindlimb (Table 1). Duty factor was not significantly different among size classes in the forelimb, whereas it was higher in the large size class than the small size class in the hindlimb (Table 1). The minimum duty factor was lower in smaller size classes in the forelimb (0.56, 0.61 and 0.67 for small, medium and large size classes) and the hindlimb (0.63, 0.70 and 0.76 for small, medium and large size classes). Normalized stride lengths were longer in the small size class: significant differences were found between the small and medium size classes in the forelimb and hindlimb (Table 1).

Limb joint angles during mid-stance were also size-dependent in alligators (Fig. 2). All angles, except humerus and femur retraction–protraction, elbow flexion and wrist plantarflexion angles, showed some differences between size classes (Table 2). The humerus and femur were more adducted in the medium and large size classes than in the small size class, as pairwise comparisons showed significant or nearly significant differences between these larger size classes and the small size class (Fig. 3A–C,G–I, Table 2). Degrees of humeral axial rotation were larger in the small size class than in the large and medium size classes, whereas those of femoral rotation were larger in the medium size class than in the small and large size classes (Fig. 3A–C,G–I, Table 2). The knee and ankle were less flexed in the medium and large size classes than in the small size class (Fig. 3J–L, Table 2). More abducted shoulder and hip and flexed knee and ankle in the small size class were reflected in its lower shoulder and hip height profiles (Fig. 3M–O). The shoulder and hip height profiles overlapped during stance in the small size

Table 1. Comparisons of speed and stride parameters among three size classes of American alligator

|	Dimensionless speed [$u(\boldsymbol{g}{\cdot}h)^{-0.5}$]	Stride duration (s)	Duty factor	Stride length (BLU)
Forelimb				
Small size class	0.194±0.008	1.226±0.041	0.718±0.012	0.347±0.011
Medium size class	0.138±0.012	1.943±0.117	0.722±0.010	0.246±0.006
Large size class	0.128±0.010	2.573±0.155	0.734±0.013	0.291±0.006
LME model Ω^2	0.277	0.872	0.022	0.591
ANOVA P	0.001	0.004	0.817	0.002
Small vs medium z	4.239	−1.479	0.164	4.249
Small vs large z	4.363	−4.013	−0.406	1.709
Medium vs large z	0.639	−2.988	−0.615	−1.512
Small vs medium P	<0.001	0.298	0.985	<0.001
Small vs large P	<0.001	<0.001	0.913	0.199
Medium vs large P	0.798	0.008	0.811	0.282
Hindlimb				
Small size class	0.176±0.009	1.416±0.063	0.740±0.012	0.373±0.014
Medium size class	0.144±0.010	1.873±0.116	0.788±0.008	0.262±0.005
Large size class	0.104±0.009	3.146±0.226	0.834±0.009	0.285±0.004
LME model Ω^2	0.347	0.835	0.560	0.679
ANOVA P	0.001	0.001	0.015	0.005
Small vs medium z	2.541	0.054	−2.030	3.704
Small vs large z	5.641	−4.559	−3.099	1.971
Medium vs large z	3.096	−5.376	−1.638	−0.786
Small vs medium P	0.030	0.998	0.104	0.001
Small vs large P	<0.001	<0.001	0.005	0.117
Medium vs large P	0.005	<0.001	0.228	0.709

Linear mixed effects (LME) models were used with size class and dimensionless speed [$u(\boldsymbol{g}{\cdot}h)^{-0.5}$, where u is walking speed, $\boldsymbol{g}$ is the acceleration of gravity and h is the extended hip to ankle length] as fixed effects and individual as a random effect. For the comparison of dimensionless speed, only size class was used as a fixed effect. The effect of size class was tested by ANOVA comparing the models with and without size class as a fixed effect. BLU, body length unit. See Materials and Methods for sample sizes in each size class. Means are presented ±s.e.m.

class, whereas the hip was higher than the shoulder during stance in the medium and large size classes.

The forelimb and hindlimb were primarily used for braking and propulsion, respectively, while both the forelimb and hindlimb produced medial forces during stance (Fig. 4). Comparisons of normalized peak forces showed that peak vertical forces of the forelimb were larger in the small size class than the medium and large size classes, whereas those of the hindlimb were larger in the medium and large size classes than the small size class (Fig. 4, Table 3). Peak propulsive, braking and medial forces in the forelimb were smaller in the medium size class than in the small size class (Fig. 4, Table 3). No significant difference among size classes was found for the hindlimb peak propulsive, braking and medial forces. GRF was directed nearly vertically at midstance for both limbs and all size classes (Table 3). Medial inclination of the GRF at midstance was similar across the size classes for the forelimb, averaging approximately 8–9 deg. For the hindlimb, medial inclination of the GRF varied slightly more across size classes, with smaller individuals showing more inclined forces than larger ones, but still averaging only 7–11 deg across the groups.

Shoulder protraction and abduction, humerus external rotation, elbow flexion and wrist dorsiflexion moments dominated for the forelimb, and hip retraction and abduction, knee flexion and ankle dorsiflexion moments dominated for the hindlimb during stance (Fig. 5). Comparisons of normalized peak joint moments showed that peak shoulder protraction and abduction moments were generally larger in the small size class than the medium and large size classes, and peak hip retraction and abduction moments were larger in the small size class than in the medium size class (Fig. 5A–C,G–I, Table 4). Peak humeral and femoral internal rotation moments were smaller in the medium size class than either the small or large size classes (Table 4). Peak elbow flexion moments were larger in the small and large size classes than the medium size class, and peak knee flexion moments were larger in the large size class than the small and medium size classes (Fig. 5D–F,J–L, Table 4). No significant difference among size
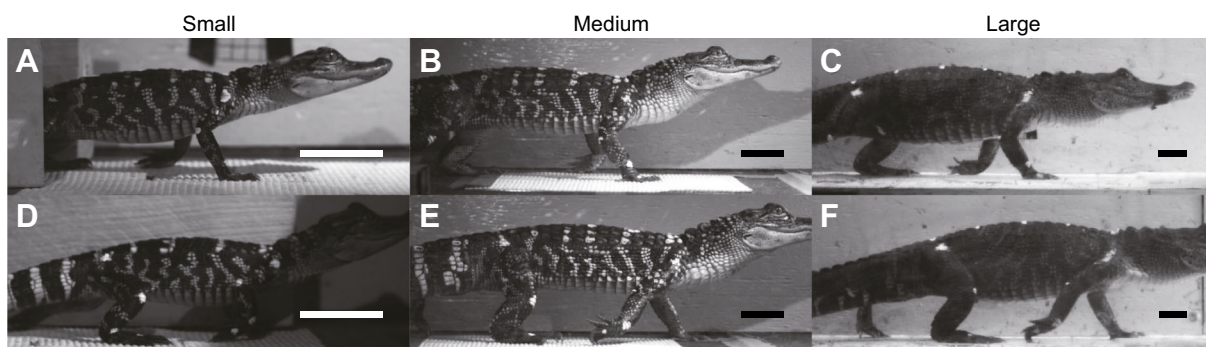
Fig. 2. Comparisons of mid-stance limb posture among three size classes of American alligators. (A–C) Forelimb posture and (D–F) hindlimb posture for small, medium and large alligators (from left to right). Scale bars are 5 cm.

Table 2. Comparisons of forelimb and hindlimb joint angles among three size classes of American alligator

Forelimb	Humerus retraction–protraction angle (deg) (max–min)	Humerus adduction angle (deg) (mean)	Humerus long axis rotation (deg) (max–min)	Elbow flexion angle (deg) (mean)	Wrist plantarflexion angle (deg) (mean)
Small size class	92.0±2.0	−25.9±1.7	68.2±2.6	86.3±2.5	−24.0±2.0
Medium size class	87.4±1.8	−39.3±1.4	39.6±2.3	84.8±1.5	−16.3±0.7
Large size class	85.6±2.2	−40.9±1.2	47.5±2.7	84.7±2.0	−15.4±1.1
LME model Ω^2	0.200	0.702	0.545	0.288	0.399
ANOVA P	0.241	0.011	<0.001	0.753	0.068
Small vs medium z	−1.089	−2.771	−8.406	−0.603	1.967
Small vs large z	−1.268	−2.212	−5.591	−0.507	1.663
Medium vs large z	0.444	0.273	−1.864	0.076	−0.212
Small vs medium P	0.518	0.015	<0.001	0.816	0.118
Small vs large P	0.410	0.067	<0.001	0.866	0.216
Medium vs large P	0.896	0.959	0.148	0.997	0.975

Hindlimb	Femur retraction–protraction angle (deg) (max–min)	Femur adduction angle (deg) (mean)	Femur long axis rotation (deg) (max–min)	Knee flexion angle (deg) (mean)	Ankle dorsiflexion angle (deg) (mean)
Small size class	95.9±3.3	−42.5±1.5	26.1±1.3	83.0±2.2	131.3±1.4
Medium size class	87.3±3.1	−55.0±1.6	42.7±1.6	60.1±1.9	112.2±1.6
Large size class	95.7±2.0	−54.8±0.8	33.2±1.2	71.2±1.5	120.7±1.5
LME model Ω^2	0.556	0.659	0.612	0.624	0.617
ANOVA P	0.651	0.008	<0.001	<0.001	<0.001
Small vs medium z	−0.428	−3.157	7.852	−6.541	−7.038
Small vs large z	0.367	−2.359	1.477	−3.143	−3.537
Medium vs large z	−0.679	0.059	5.815	−1.998	−2.119
Small vs medium P	0.903	0.005	<0.001	<0.001	<0.001
Small vs large P	0.927	0.047	0.300	0.005	0.001
Medium vs large P	0.773	0.998	<0.001	0.111	0.085

Larger absolute values indicate larger angles of interest. Mean angles were taken from 25–75% of stance. LME models were used with size class and dimensionless speed as fixed effects and individual as a random effect. The effect of size class was tested by ANOVA comparing the models with and without size class as a fixed effect. See Materials and Methods for sample sizes in each size class. Means are presented ±s.e.m.

classes was found for humeral and femoral external rotation moments or wrist and ankle dorsiflexion moments (Table 4). Sensitivity analyses of peak forelimb and hindlimb joint moments using either the dorsal, ventral, anterior or posterior edge of each forelimb and hindlimb joint landmark (3.4–9.3 mm diameter) in a representative trial (al09f21) showed that landmark-dependent errors for dominant joint moments (>0.05 N·m kg$^{-4/3}$) averaged less than 20% from the original estimates that used the center of each landmark (Table S1), providing confidence that the patterns we identified are robust to digitizing error from marker placement or skin motion over a joint.

The CoM shifts from juveniles through subadults in alligators. CoM is positioned in the mid-torso (CoM$_{SH}$ 57–62%) in the small size class (0.23–0.26 kg), moves posteriorly near the hip (CoM$_{SH}$ 65–80%) in the medium size class (0.68–2.80 kg), and then moves back anteriorly (CoM$_{SH}$ 64–72%) in the large size class (3.71–8.00 kg) (Fig. 6A).

DISCUSSION
Larger alligators walked slowly with longer stride durations. Mean duty factors did not differ significantly across size classes, except between small and large animals for the hindlimb (Table 1); however, the minimum duty factor was higher in larger size classes for the forelimb and hindlimb (see Results). Slower movement of larger alligators would allow them to distribute forces over a longer stance duration, and reduce peak muscle and bone stresses (Alexander et al., 1979b; Dick and Clemente, 2017).

Ontogenetic changes in limb posture and their mechanical consequences
Comparisons of limb posture among juvenile to subadult alligators revealed that larger size classes use a more adducted humerus and femur, a less flexed knee and a less dorsiflexed ankle than the small

size class (Figs 2 and 3, Table 2). The ontogenetic shift from more sprawled and crouched posture to more upright posture in alligators is comparable to the interspecific trend in quadrupedal mammals – larger mammals use more upright limb posture than smaller ones at the speed of the trot–gallop transition (Biewener, 1989, 1990). Consequently, forelimb and hindlimb muscle EMA (ratio of the muscle moment arm to the GRF moment arm) in large mammals is higher than that in smaller mammals with more crouched limb posture (Biewener, 1989, 1990). Positive scaling of limb muscle EMA against mass has been observed in phylogenetically diverse lineages, and similar scaling relationships have been found among more restricted groups (i.e. cercopithecine primates and rodents; Biewener, 2005; Polk, 2002). Notable exceptions to the mammalian trend are felids, where limb posture does not largely change across a 50-fold range in mass (Day and Jayne, 2007). However, the EMA of the elbow and knee extensors may scale positively among felids owing to positive scaling of the muscle moment arms (Harper and Sylvester, 2019), which requires further testing. Overall positive scaling of the limb muscle EMA in mammals allows them to keep up with the demands for muscle force production while maintaining muscle and bone stresses over a range of mass, though large erect animals may sacrifice a cost in acceleration and maneuverability (Biewener, 1989, 1990; Cuff et al., 2016; Gray, 1968). In contrast to quadrupedal mammals with parasagittal limb posture, varanid lizards with non-parasagittal limb posture do not appear to change hindlimb posture during running over a size range of 0.04–7.9 kg (Clemente et al., 2011). Conceivably, hindlimb muscle EMA may decrease with more upright posture in varanids, and they may reduce limb bone stresses by minimizing internal rotation of the femur at mid-stance (Clemente et al., 2011).

The similarity of postural shifts during ontogeny in alligators and across mass in mammals, but not varanids, is not easy to explain. Counterintuitively, *in vivo* and theoretical studies indicated that
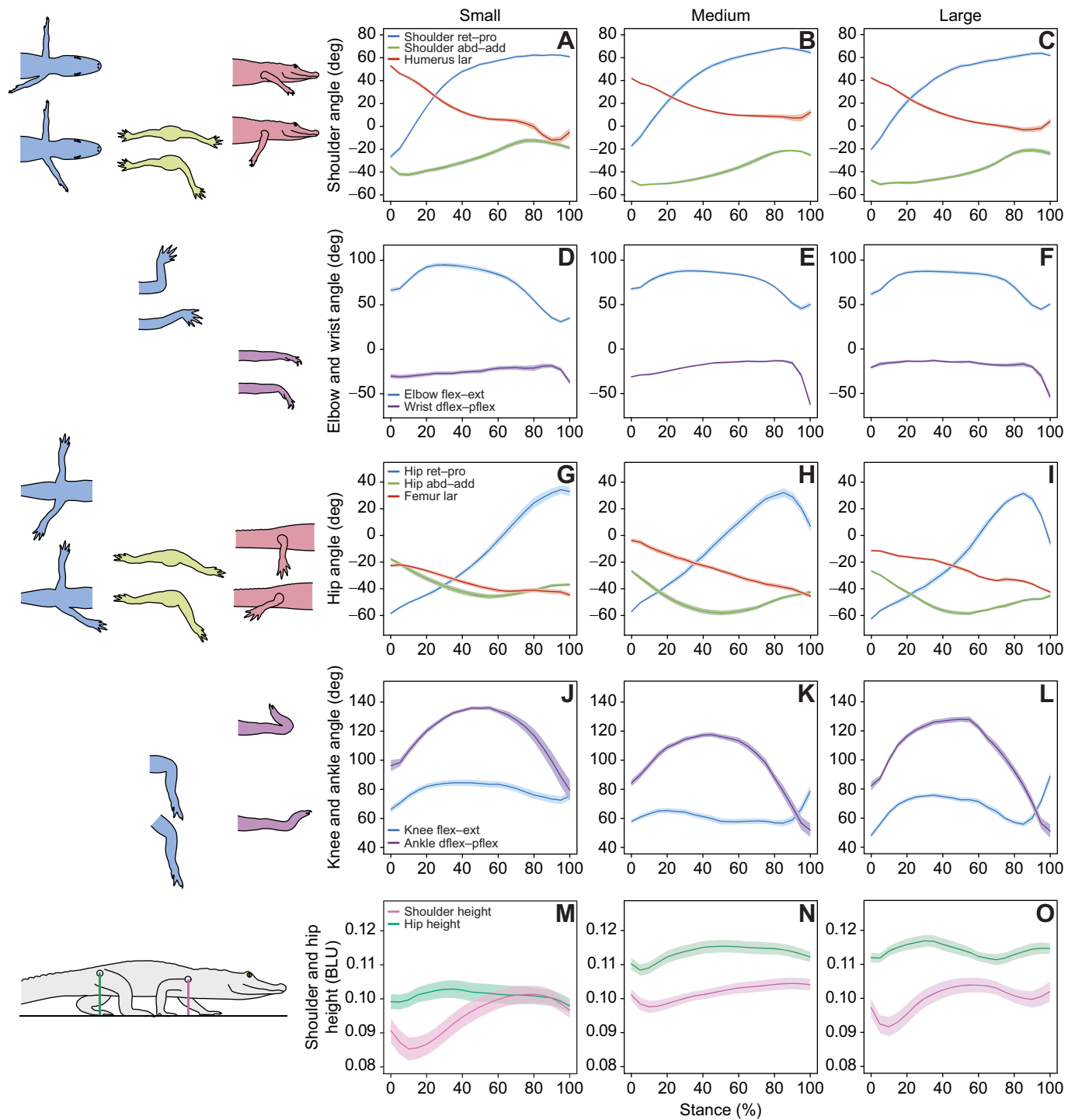
Fig. 3. Forelimb and hindlimb joint angles and shoulder and hip heights throughout stance in three size classes of American alligators. (A–C) Shoulder angles, (D–F) elbow and wrist angles, (G–I) hip angles, (J–L) knee and ankle angles, and (M–O) shoulder and hip heights in body length unit (BLU). Lines and shaded areas represent mean traces and their standard errors, respectively. Note that humerus and femur long axis rotation are affected by elbow and knee abduction–adduction that was not accounted for, and flexion–extension axes of the elbow, wrist, knee and ankle change with respect to osteologically defined joint axes during stance. Limb movement abbreviations: abd, abduction; add, adduction; dflex, dorsiflexion; ext, extension; flex, flexion; lar, long axis rotation; pflex, plantarflexion; pro, protraction; ret, retraction. See Materials and Methods for sample sizes for each size class.

hindlimb bone stresses increase as individual American alligators select the use of more upright hindlimb posture (Blob and Biewener, 1999, 2001). During the use of more upright stance by animals in a size range between the medium and large animals of the current study, an anterior shift in the CoP of the hindfoot increased the

moment arm of the GRF about the ankle (Blob and Biewener, 2001). This increased ankle flexion moment was hypothesized to be countered by a chain of increased muscle activation and force production spanning from the ankle extensors that cross the ankle and knee joints to the knee extensor muscles, inducing higher
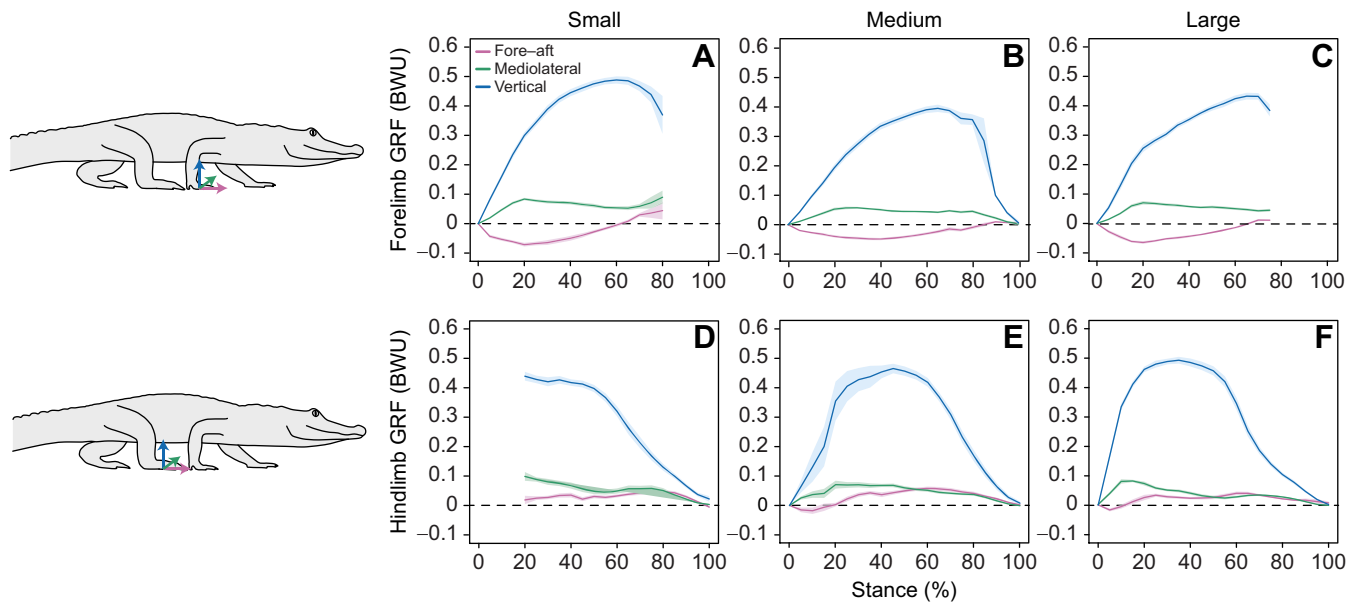
Fig. 4. Forelimb and hindlimb forces throughout stance in three size classes of American alligators. (A–C) Forelimb and (D–F) hindlimb GRF in body weight unit (BWU). Lines and shaded areas represent mean traces and their standard errors, respectively. See Materials and Methods for sample sizes for each size class.

dorsoventral bending stress in the femur (Blob and Biewener, 2001; Reilly and Blob, 2003). Comparisons of electromyographic burst intensities of stance phase muscles at different femoral adduction angles revealed more intense bursts of ankle and knee extensors during more upright steps, supporting the chain of muscle activation hypothesis (Reilly and Blob, 2003). However, our ontogenetic comparisons of limb posture and joint moments in alligators did not provide a simple parallel to the patterns from these previous

observations of postural change by medium-sized individuals. Although hindlimb posture was more upright in the medium and large classes than the small class, normalized ankle and knee flexion moments were not different among size classes, except the larger knee flexion moment of the large class compared with other classes (Table 4). To better understand the differences between these analyses, we took the separate data from each individual alligator in this study and conducted a least squares regression of ankle

Table 3. Comparisons of peak forelimb and hindlimb forces and GRF medial inclination angles among three size classes of American alligator

	Peak vertical force (BWU)	Peak propulsive force (BWU)	Peak braking force (BWU)	Peak medial force (BWU)	GRF medial inclination angle (deg)
Forelimb					
Small size class	0.510±0.011	0.040±0.005	−0.098±0.007	0.114±0.005	8.1±0.5
Medium size class	0.413±0.010	0.007±0.002	−0.059±0.004	0.071±0.004	8.5±0.4
Large size class	0.441±0.011	0.025±0.003	−0.075±0.003	0.080±0.005	8.7±0.6
LME model Ω^2	0.385	0.315	0.297	0.523	0.108
ANOVA P	<0.001	0.002	0.002	0.006	0.397
Small vs medium z	5.560	4.999	−3.882	3.326	−0.796
Small vs large z	3.370	2.004	−1.693	1.797	−0.958
Medium vs large z	−1.503	−2.484	1.688	−0.797	−0.339
Small vs medium P	<0.001	<0.001	<0.001	0.003	0.704
Small vs large P	0.002	0.111	0.207	0.169	0.601
Medium vs large P	0.289	0.035	0.209	0.703	0.938
Hindlimb					
Small size class	0.461±0.012	0.072±0.006	−0.016±0.003	0.116±0.012	11.0±1.2
Medium size class	0.507±0.015	0.074±0.006	−0.011±0.003	0.094±0.005	9.0±1.0
Large size class	0.517±0.009	0.068±0.008	−0.011±0.003	0.070±0.005	6.8±0.6
LME model Ω^2	0.174	0.094	0.051	0.259	0.144
ANOVA P	0.019	0.619	0.521	0.090	0.033
Small vs medium z	−2.778	−0.647	−0.996	1.163	1.596
Small vs large z	−3.069	−0.639	−0.745	1.850	2.829
Medium vs large z	−0.835	−0.126	0.079	0.995	1.691
Small vs medium P	0.015	0.793	0.577	0.473	0.246
Small vs large P	0.006	0.797	0.735	0.152	0.013
Medium vs large P	0.680	0.991	0.997	0.578	0.207

GRF medial inclination angles were taken from 25–75% of stance. LME models were used with size class and dimensionless speed as fixed effects and individual as a random effect. The effect of size class was tested by ANOVA comparing the models with and without size class as a fixed effect. BWU, body weight unit. See Materials and Methods for sample sizes in each size class. Means are presented ±s.e.m.
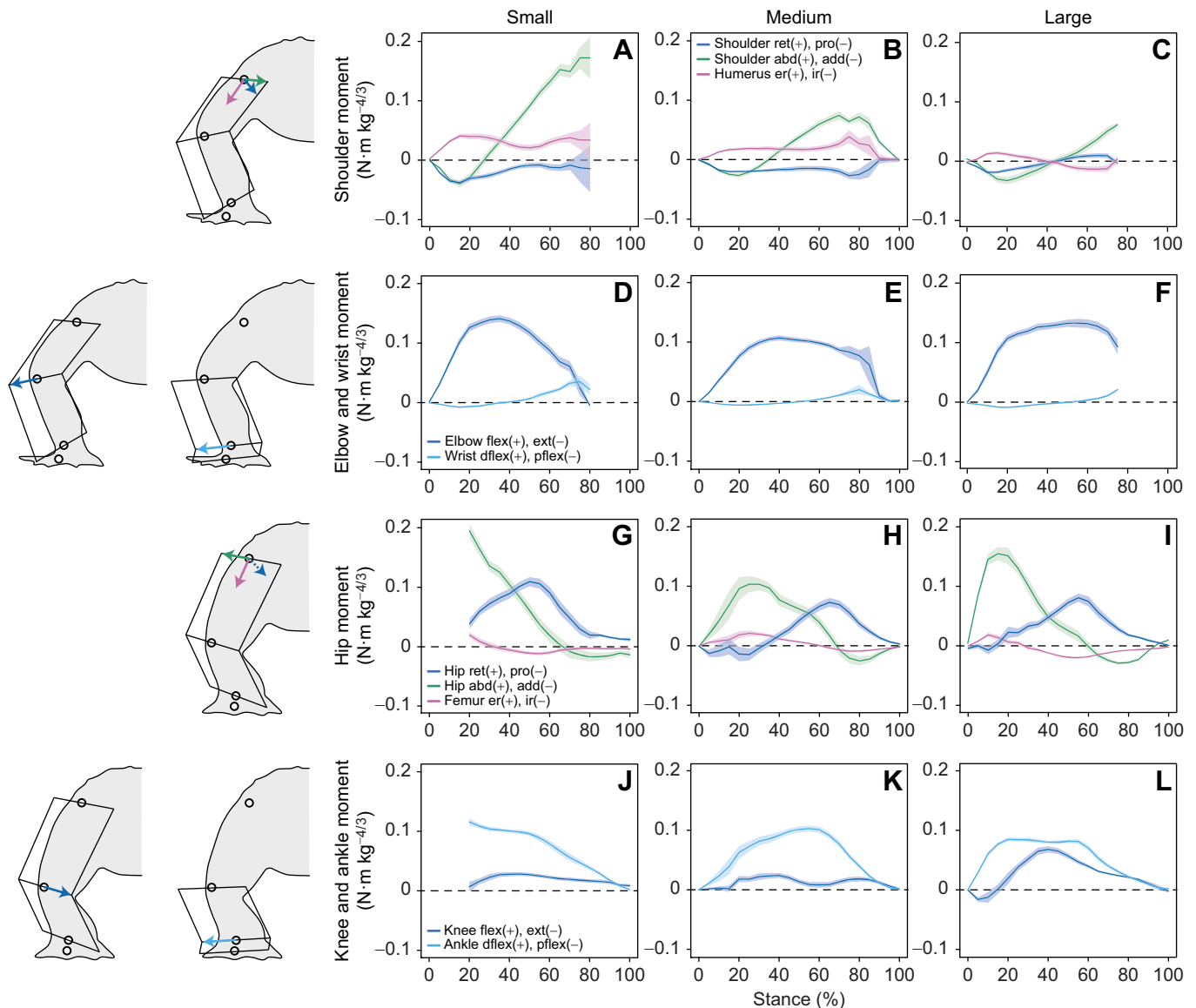
Fig. 5. Forelimb and hindlimb joint moments exerted by the GRF throughout stance in three size classes of American alligators. (A–C) Shoulder moments, (D–F) elbow and wrist moments, (G–I) hip moments and (J–L) knee and ankle moments. Moments are in normalized units (N·m kg$^{-4/3}$). Lines and shaded areas represent mean traces and their standard errors, respectively. Joint moment abbreviations: abd, abduction; add, adduction; dflex, dorsiflexion; er, external rotation; ext, extension; flex, flexion; ir, internal rotation; pflex, plantarflexion; pro, protraction; ret, retraction. See Materials and Methods for sample sizes for each size class.

dorsiflexion moment on femoral adduction angle. Interpretations should be made cautiously given our small sample sizes of trials for some individuals; however, within each individual alligator, more adducted (upright) femoral postures also showed greater ankle dorsiflexion moments, with regressions indicating significant or nearly significant correlations for two of seven individuals (Table S2). These results further suggest that the consequences of postural change within an animal at a particular body size may differ from consequences of postural change compared across different body sizes.

Differing impacts of postural change across gradients of body size are likely related to allometric growth of body and limb proportions and their consequences for joint moments among size classes. Based on the measurement datasets of Farlow et al. (2005) and Iijima and Kubo (2019), length percentages of the femur to the hindlimb (sum of the femur, tibia and metatarsal III) would be 35.8, 40.4 and 42.6%,

respectively, and those of the hindlimb to presacral vertebrae would be 72.0, 66.6 and 63.0%, for the average sizes of the small, medium and large size classes, respectively. Owing to the shorter hindlimb and distal segments (tibia and metatarsal III) within the hindlimb, larger alligators might incur smaller normalized joint moments about the ankle and knee. Therefore, the chain activation of the ankle and knee flexors (Blob and Biewener, 2001; Reilly and Blob, 2003) would be mitigated in larger alligators.

The use of more upright limb posture in larger alligators could have mechanical benefits in the context of the muscle forces exerted in the forelimb and hindlimb. Limb muscle masses and cross-sectional areas generally scale with overall geometric similarity in American alligators (Allen et al., 2010), so it would be increasingly challenging for larger alligators to support their weights unless changes in limb posture or proportions allow them to reduce joint moments. Indeed, larger alligators used more adducted forelimb and

Table 4. Comparisons of peak forelimb and hindlimb joint moments among three size classes of American alligator

| Forelimb	Shoulder protraction moment	Shoulder abduction moment	Humerus external rotation moment	Humerus internal rotation moment	Elbow flexion moment	Wrist dorsiflexion moment
Small size class	−0.050±0.004	0.169±0.009	0.055±0.005	−0.009±0.003	0.154±0.006	0.030±0.004
Medium size class	−0.029±0.002	0.086±0.005	0.032±0.004	−0.003±0.002	0.117±0.004	0.012±0.002
Large size class	−0.020±0.002	0.051±0.006	0.019±0.003	−0.018±0.004	0.139±0.007	0.015±0.003
LME model Ω^2	0.507	0.756	0.462	0.148	0.259	0.259
ANOVA P	0.016	0.004	0.032	0.016	0.001	0.047
Small vs medium z	2.229	3.088	−1.709	1.653	−4.228	−2.272
Small vs large z	2.603	3.127	−2.239	−1.688	−1.395	−1.369
Medium vs large z	−0.911	−0.903	0.952	3.356	−2.440	−0.426
Small vs medium P	0.065	0.006	0.199	0.223	<0.001	0.059
Small vs large P	0.025	0.005	0.064	0.209	0.342	0.355
Medium vs large P	0.631	0.635	0.604	0.002	0.039	0.904
Hindlimb	Hip retraction moment	Hip abduction moment	Femur external rotation moment	Femur internal rotation moment	Knee flexion moment	Ankle dorsiflexion moment
Small size class	0.119±0.006	0.175±0.009	0.015±0.003	−0.021±0.003	0.040±0.002	0.112±0.003
Medium size class	0.083±0.007	0.117±0.008	0.024±0.003	−0.011±0.002	0.039±0.004	0.109±0.004
Large size class	0.090±0.007	0.152±0.008	0.014±0.002	−0.022±0.002	0.075±0.005	0.094±0.003
LME model Ω^2	0.301	0.311	0.192	0.333	0.498	0.425
ANOVA P	0.030	0.001	0.086	0.005	0.001	0.547
Small vs medium z	−2.402	4.683	1.560	3.259	−0.361	−0.096
Small vs large z	−1.146	2.012	−0.084	0.469	4.114	−0.801
Medium vs large z	−0.747	2.045	1.361	2.249	−4.819	0.744
Small vs medium P	0.043	<0.001	0.260	0.003	0.930	0.995
Small vs large P	0.483	0.108	0.996	0.885	<0.001	0.699
Medium vs large P	0.733	0.101	0.359	0.062	<0.001	0.735

Normalized joint moments (N·m kg$^{-4/3}$) were compared. Larger absolute values indicate larger moments of interest. LME models were used with size class and dimensionless speed as fixed effects and individual as a random effect. The effect of size class was tested by ANOVA comparing the models with and without size class as a fixed effect. See Materials and Methods for sample sizes in each size class. Means are presented ±s.e.m.

hindlimb posture, and their normalized shoulder and hip abduction moments were reduced, which would be expected to require lower levels of recruitment for shoulder and hip adductor muscles during stance (Figs 3 and 5, Tables 2 and 4). Furthermore, large individuals of other crocodylian species also commonly walk with upright limb posture (Cott, 1961; Farlow et al., 2018) with the exception of Indian gharials, the most aquatic extant crocodylians that possess considerably shortened limbs (Bustard and Singh, 1977; Iijima et al., 2018; Singh and Bustard, 1976).

Ontogenetic changes in limb posture have been observed in some species of mammals and lizards. Domestic cats and vervet monkeys show more flexed limbs in the first few weeks after birth owing to their immature neuromuscular system and lack of stability (Howland et al., 1995; Peters, 1983; Vilensky and Gankiewicz, 1989). Similarly, forelimbs and hindlimbs of certain dog breeds (e.g. beagles), and the hindlimbs of horses, become slightly more erect as juveniles grow to adult size (Grossi and Canals, 2010; Helmsmüller et al., 2014). Other studies have highlighted various ontogenetic trends in forelimb and hindlimb joint angles that are associated with changes in limb proportions, CoM, limb force distribution and limb function, as well as mass (Burgess et al., 2016; Patel et al., 2013; Young, 2009, 2012; Young and Shapiro, 2018; Zeininger et al., 2017). As for lizards, desert iguanas change limb posture through ontogeny, where adults use more crouched posture than juveniles at the speed of the walk–run transition (Irschick and Jayne, 2000). However, more extended limb posture in juvenile desert iguanas might be explained by their significantly longer limbs as compared with adults (Irschick and Jayne, 2000), which would increase joint moments if the same limb joint angles were used as in adults (Polk, 2002). In American alligators, the smallest individuals that we examined showed steady and stable steps; thus, an underdeveloped neuromuscular system should not be the cause of their flexed limb posture. Moreover, alligators show negative

scaling of hindlimb length against trunk length as in desert iguanas, but the scaling exponent is closer to 1 and allometric morphological changes are smaller (Dodson, 1975; Farlow and Britton, 2000; Iijima and Kubo, 2019).

Ontogenetic changes in limb posture in alligators involve alterations of not only humerus and femur adduction and the knee and ankle flexion angles, but also degrees of humerus and femur long axis rotation during stance. In the forelimb, the medium and large classes that use a more adducted humerus also showed smaller degrees of humeral axial rotation than the small size class, owing to lesser external rotation at the touchdown of the manus and lesser internal rotation at its lift-off (Fig. 3A–C, Table 2). Meanwhile, in the hindlimb, the medium and large size classes that walked with a more adducted femur showed greater degrees of femoral axial rotation than the small class owing to lesser internal rotation at foot touchdown (Fig. 3G–I, Table 2). Previous studies of forelimb and hindlimb kinematics in sprawling to erect quadrupeds, including salamanders, lizards, crocodylians, opossums and rats, have suggested such an association between greater adduction and lesser degrees of humerus and femur axial rotation during stance (Baier and Gatesy, 2013; Bakker, 1971; Bonnan et al., 2016; Gatesy, 1991; Irschick and Jayne, 1999; Jenkins, 1971; Karakasiliotis et al., 2013; Nyakatura et al., 2014; 2019; Sullivan, 2007). The association of greater humeral adduction and lesser humeral axial rotation in alligators matches expectations from other taxa, but the finding of greater femoral adduction and greater femoral axial rotation was unexpected. Even with more erect limb posture, internal rotation of the femur may play an important role during stance in alligators, given the potential for a strong internal rotation moment about the femoral long axis exerted by the femoral retractor M. caudofemoralis longus (CFL) (Blob, 2000; Gatesy, 1990, 1997; Reilly et al., 2005). However, some debate about this possibility also exists, as CFL has been regarded as an external rotator of the femur
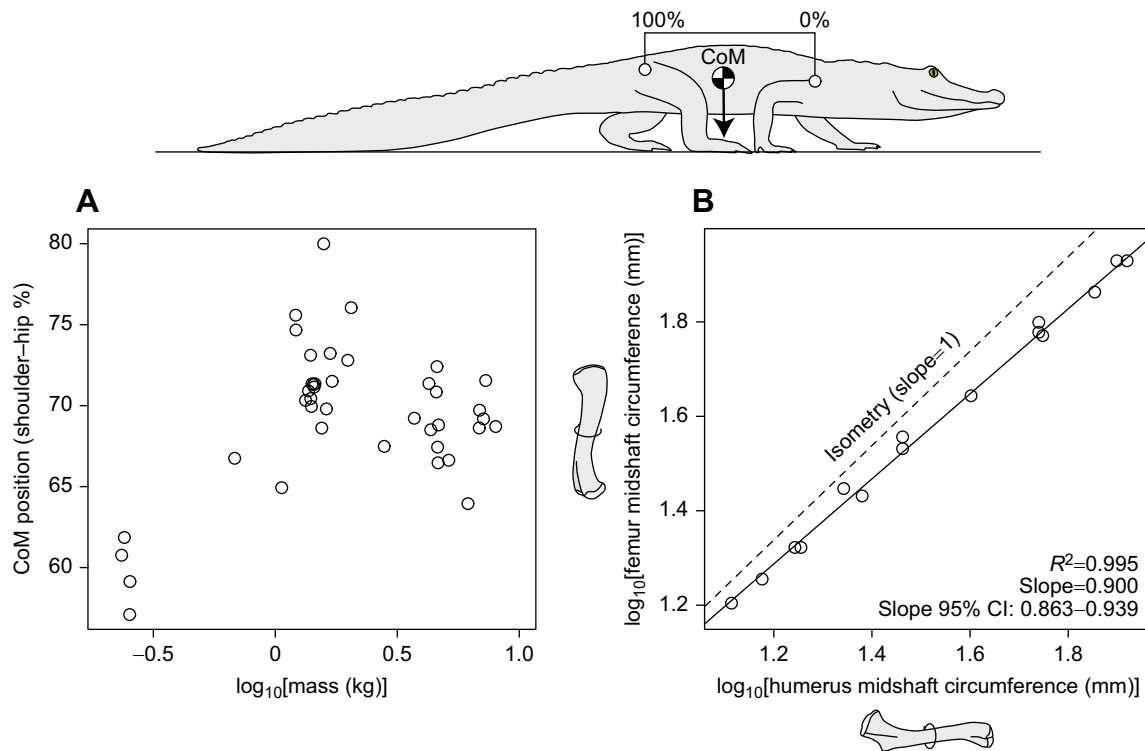
Fig. 6. Ontogenetic changes in the center of mass (CoM) and limb morphology in American alligators. (A) CoM position (shoulder–hip %) versus body mass and (B) femur versus humerus midshaft circumferences. Each data point in A represents a single individual (n=40). Data depicted in B are from Iijima and Kubo (2019).

in some recent studies of crocodylians (Allen et al., 2021; Wiseman et al., 2021).

Ontogenetic changes in the CoM and limb force distribution

Additional intriguing aspects of locomotor ontogeny in alligators besides postural shifts are changes in the CoM and forelimb and hindlimb force distribution. The CoM is positioned more anteriorly in small individuals (Fig. 6A). During ontogeny, the CoM shifts backward from the small (0.23–0.26 kg) through medium (0.68–2.80 kg) size classes, and then shifts slightly forward from the medium (0.68–2.80 kg) through large (3.71–8.00 kg) size classes. The more anteriorly positioned CoM in the small size class coincided with their higher forelimb and lower hindlimb normalized peak vertical forces as compared with larger size classes (Fig. 4, Table 3). Nonetheless, division of labor was maintained throughout the size classes, where the forelimb and hindlimb produced net braking and propulsive forces, respectively (Fig. 4).

Limb force distribution varies among quadrupeds. In mammals, peak vertical forces are forelimb dominant in non-primates including rats, cats, horses, giraffes, bears and elephants (Basu et al., 2019; Granatosky et al., 2018; Merkens et al., 1985; Ren et al., 2010; Shine et al., 2015; Zumwalt et al., 2006), but hindlimb dominant in most primates (Demes et al., 1994; Kimura et al., 1979). It should also be noted that peak forces and impulses become increasingly hindlimb dominant with higher running speeds in some cursorial mammals (Hudson et al., 2012; Self Davies et al., 2019). Among amphibians and reptiles, vertical forces are potentially forelimb dominant in subadult spectacled caimans (Nyakatura et al., 2019), hindlimb dominant in varanid lizards and juvenile American alligators (Cieri et al., 2021; Willey et al., 2004), evenly distributed between the forelimb and hindlimb in Indo-Pacific geckos (Chen et al., 2006), and exhibit various patterns across salamanders and

multiple lizard families (Kawano et al., 2016; McElroy et al., 2014; Nyakatura et al., 2019). Limb force distribution also varies intraspecifically. Decreases in relative forelimb versus hindlimb peak vertical forces, together with the caudal shift of the CoM, occur during ontogeny in primates (Druelle et al., 2017; Grand, 1983; Turnquist and Wells, 1994; Young, 2012). In contrast, forelimbs become more dominant weight supporters during postnatal weeks 11–51 in dogs such as beagles, because more retracted forelimbs place the forefeet closer to the CoM, and abdominal organs grow with negative allometry (Helmsmüller et al., 2014). However, in a different breed of dogs, relative forelimb versus hindlimb peak vertical forces decreased during postnatal weeks 4–15, but remained unchanged in adults (Biknevicius et al., 1997). Furthermore, interspecific allometry of limb force distribution was reported in varanid lizards, where allometric exponents of peak vertical forces and vertical impulses were larger for the hindlimb than for the forelimb, and the CoM was more caudally positioned in larger species (Cieri et al., 2021).

Forelimb dominance of peak vertical forces in small alligators is explained by not only their more anteriorly positioned CoM, but also their compliant hindlimbs. In small alligators, stance phase was characterized by more flexed hindlimbs than forelimbs, and by smaller vertical oscillation of the hip than the shoulder. Compliant walking is known to lengthen stance duration, flatten the profile and reduce the peaks of vertical forces, but increase mechanical cost (McMahon et al., 1987; Ren et al., 2010; Schmitt, 1999; Schmitt and Hanna, 2004; Young, 2012). Additionally, though we did not examine whole-body mechanics, more compliant hindlimbs in small alligators are expected to reduce energy recovery through the inverted pendulum mechanism (Willey et al., 2004). Given these disadvantages, reasons as to why small alligators (total length ~0.5 m, body mass ~0.3 kg) walk with compliant hindlimbs remain

uncertain. One possibility (suggested by a reviewer of this paper) could be that using more flexed hindlimbs may allow the hindlimb extensor muscles to operate at longer fascicle lengths that could improve their shortening velocity and capacity for mechanical work. Such advantages for mechanical power generation in the hindlimbs could be significant for smaller alligators, which likely face a greater risk of predation and could benefit from accelerating their body away from threats.

The anterior shift of the CoM from the medium (0.68–2.80 kg) through large (3.71–8.00 kg) size classes most likely continues through adult size in alligators owing to the allometric growth of their body segments. In American alligators, many of the jaw adductor muscle masses scale with positive allometry against snout–vent lengths, which enables positive scaling of bite force (Erickson et al., 2003; Gignac and Erickson, 2016). Furthermore, in non-gavialid crocodylians including American alligators, forelimbs grow faster than hindlimbs; thus, larger individuals have increasingly longer and thicker forelimb bones (Iijima and Kubo, 2019) (Fig. 6B). A relatively heavier head and forelimbs would together place the CoM more anteriorly in larger alligators, which is in accord with the craniodorsal CoM shift in juvenile to adult freshwater crocodiles estimated by computational modeling (Allen et al., 2009). Future studies of terrestrial locomotion among full-size adult alligators could give further insights into how animals with non-parasagittal limb posture modulate limb joint angles, joint moments and limb force distribution as they increase mass and change in body proportions and inertial properties. Such empirical data on size-dependent changes in the locomotion of crocodylians could provide a basis for discussing the evolution of body size and erect limb posture in early archosauriforms.

References
Alexander, R. M. N., Jayes, A. S., Maloiy, G. M. O. and Wathuta, E. M. (1979a). Allometry of the limb bones of mammals from shrews (*Sorex*) to elephant (*Loxodonta*). *J. Zool.* **189**, 305-314. doi:10.1111/j.1469-7998.1979.tb03964.x

Alexander, R. M. N., Maloiy, G. M. O., Hunter, B., Jayes, A. S. and Nturibi, J. (1979b). Mechanical stresses in fast locomotion of buffalo (*Syncerus caffer*) and

elephant (*Loxodonta africana*). *J. Zool.* **189**, 135-144. doi:10.1111/j.1469-7998. 1979.tb03956.x

Alexander, R. M. N., Jayes, A. S., Maloiy, G. M. O. and Wathuta, E. M. (1981). Allometry of the leg muscles of mammals. *J. Zool.* **194**, 539-552. doi:10.1111/j. 1469-7998.1981.tb04600.x

Allen, V., Paxton, H. and Hutchinson, J. R. (2009). Variation in center of mass estimates for extant sauropsids and its importance for reconstructing inertial properties of extinct archosaurs. *Anat. Rec.* **292**, 1442-1461. doi:10.1002/ar. 20973

Allen, V., Elsey, R. M., Jones, N., Wright, J. and Hutchinson, J. R. (2010). Functional specialization and ontogenetic scaling of limb anatomy in *Alligator mississippiensis*. *J. Anat.* **216**, 423-445. doi:10.1111/j.1469-7580.2009.01202.x

Allen, V. R., Kilbourne, B. M. and Hutchinson, J. R. (2021). The evolution of pelvic limb muscle moment arms in bird-line archosaurs. *Sci. Adv.* **7**, eabe2778. doi:10. 1126/sciadv.abe2778

Baier, D. B. and Gatesy, S. M. (2013). Three-dimensional skeletal kinematics of the shoulder girdle and forelimb in walking *Alligator*. *J. Anat.* **223**, 462-473. doi:10. 1111/joa.12102

Bakker, R. T. (1971). Dinosaur physiology and the origin of mammals. *Evolution* **25**, 636-658. doi:10.2307/2406945

Basu, C., Wilson, A. M. and Hutchinson, J. R. (2019). The locomotor kinematics and ground reaction forces of walking giraffes. *J. Exp. Biol.* **222**, 159277. doi:10. 1242/jeb.159277

Bates, D., Mächler, M., Bolker, B. M. and Walker, S. C. (2015). Fitting linear mixed-effects models using lme4. *J. Stat. Softw.* **67**, 1-48. doi:10.18637/jss.v067.i01

Benton, M. J. and Clark, J. M. (1988). Archosaur phylogeny and the relationships of the Crocodylia. In *The Phylogeny and Classification of the Tetrapods*, Vol. 1 (ed. M. J. Benton), pp. 295-338. Oxford: Clarendon Press.

Bertram, J. E. A. and Biewener, A. A. (1990). Differential scaling of the long bones in the terrestrial Carnivora and other mammals. *J. Morphol.* **204**, 157-169. doi:10. 1002/jmor.1052040205

Biewener, A. A. (1983). Allometry of quadrupedal locomotion: the scaling of duty factor, bone curvature and limb orientation to body size. *J. Exp. Biol.* **105**, 147-171. doi:10.1242/jeb.105.1.147

Biewener, A. A. (1989). Scaling body support in mammals: limb posture and muscle mechanics. *Science* **245**, 45-48. doi:10.1126/science.2740914

Biewener, A. A. (1990). Biomechanics of mammalian terrestrial locomotion. *Science* **250**, 1097-1103. doi:10.1126/science.2251499

Biewener, A. A. (2005). Biomechanical consequences of scaling. *J. Exp. Biol.* **208**, 1665-1676. doi:10.1242/jeb.01520

Biewener, A. A. (2015). Going from small to large: mechanical implications of body size diversity in terrestrial mammals. In *Great Transformations in Vertebrate Evolution* (ed. K. P. Dial, N. Shubin and E. L. Brainerd), pp. 227-238. Chicago: University of Chicago Press.

Biewener, A. A. and Patek, S. N. (2018). *Animal Locomotion*. New York: Oxford University Press.

Biknevicius, A. R., Heinrich, R. E. and Dankoski, E. (1997). Effects of ontogeny on locomotor kinetics. *J. Morphol.* **232**, 235.

Blob, R. W. (2000). Interspecific scaling of the hindlimb skeleton in lizards, crocodilians, felids and canids: does limb bone shape correlate with limb posture? *J. Zool.* **250**, 507-531. doi:10.1111/j.1469-7998.2000.tb00793.x

Blob, R. W. and Biewener, A. A. (1999). *In vivo* locomotor strain in the hindlimb bones of *Alligator mississippiensis* and *Iguana iguana*: implications for the evolution of limb bone safety factor and non-sprawling limb posture. *J. Exp. Biol.* **202**, 1023-1046. doi:10.1242/jeb.202.9.1023

Blob, R. W. and Biewener, A. A. (2001). Mechanics of limb bone loading during terrestrial locomotion in the green iguana (*Iguana iguana*) and American alligator (*Alligator mississippiensis*). *J. Exp. Biol.* **204**, 1099-1122. doi:10.1242/jeb.204.6. 1099

Bonaparte, J. F. (1984). Locomotion in rauisuchid thecodonts. *J. Vertebr. Paleontol.* **3**, 210-218. doi:10.1080/02724634.1984.10011976

Bonnan, M. F., Shulman, J., Varadharajan, R., Gilbert, C., Wilkes, M., Horner, A. and Brainerd, E. (2016). Forelimb kinematics of rats using XROMM, with implications for small eutherians and their fossil relatives. *PLoS ONE* **11**, 1-21. doi:10.1371/journal.pone.0149377

Brinkman, D. (1980). The hind limb step cycle of *Caiman sclerops* and the mechanics of the crocodile tarsus and metatarsus. *Can. J. Zool.* **58**, 2187-2200. doi:10.1139/z80-301

Burgess, M. L., Schmitt, D., Zeininger, A., McFarlin, S. C., Zihlman, A. L., Polk, J. D. and Ruff, C. B. (2016). Ontogenetic scaling of fore limb and hind limb joint posture and limb bone cross-sectional geometry in vervets and baboons. *Am. J. Phys. Anthropol.* **161**, 72-83. doi:10.1002/ajpa.23009

Bustard, H. R. and Singh, L. A. K. (1977). Studies on the Indian gharial *Gavialis gangeticus* (Gmelin) (Reptilia, Crocodilia): change in terrestrial locomotory pattern with age. *J. Bombay Nat. Hist. Soc.* **74**, 534-537.

Butcher, M. T. and Blob, R. W. (2008). Mechanics of limb bone loading during terrestrial locomotion in river cooter turtles (*Pseudemys concinna*). *J. Exp. Biol.* **211**, 1187-1202. doi:10.1242/jeb.012989

Campione, N. E. and Evans, D. C. (2012). A universal scaling relationship between body mass and proximal limb bone dimensions in quadrupedal terrestrial tetrapods. *BMC Biol.* **10**, 1-21. doi:10.1186/1741-7007-10-60

Charig, A. J. (1972). The evolution of the archosaur pelvis and hindlimb: an explanation in functional terms. In *Studies in Vertebrate Evolution* (ed. K. A. Joysey and T. S. Kemp), pp. 121-155. Edinburgh: Oliver and Boyd.

Chen, J. J., Peattie, A. M., Autumn, K. and Full, R. J. (2006). Differential leg function in a sprawled-posture quadrupedal trotter. *J. Exp. Biol.* **209**, 249-259. doi:10.1242/jeb.01979

Christian, A. and Garland, T. (1996). Scaling of limb proportions in monitor lizards (Squamata: Varanidae). *J. Herpetol.* **30**, 219-230. doi:10.2307/1565513

Cieri, R. L., Dick, T. J. M. and Clemente, C. J. (2020). Monitoring muscle over three orders of magnitude: widespread positive allometry among locomotor and body support musculature in the pectoral girdle of varanid lizards (Varanidae). *J. Anat.* **237**, 1114-1135. doi:10.1111/joa.13273

Cieri, R. L., Dick, T. J. M., Irwin, R., Rumsey, D. and Clemente, C. J. (2021). The scaling of ground reaction forces and duty factor in monitor lizards: implications for locomotion in sprawling tetrapods. *Biol. Lett.* **17**, 20200612. doi:10.1098/rsbl.2020.0612

Clemente, C. J. (2014). The evolution of bipedal running in lizards suggests a consequential origin may be exploited in later lineages. *Evolution* **68**, 2171-2183. doi:10.1111/evo.12447

Clemente, C. J., Withers, P. C., Thompson, G. and Lloyd, D. (2011). Evolution of limb bone loading and body size in varanid lizards. *J. Exp. Biol.* **214**, 3013-3020. doi:10.1242/jeb.059345

Clemente, C. J., Withers, P. C. and Thompson, G. (2012). Optimal body size with respect to maximal speed for the yellow-spotted monitor lizard (*Varanus panoptes*; Varanidae). *Physiol. Biochem. Zool.* **85**, 265-273. doi:10.1086/665275

Cott, H. B. (1961). Scientific results of an inquiry into the ecology and economic status of the Nile crocodile (*Crocodilus niloticus*) in Uganda and Northern Rhodesia. *Trans. Zool. Soc. London* **29**, 211-356. doi:10.1111/j.1096-3642.1961.tb00220.x

Cuff, A. R., Sparkes, E. L., Randau, M., Pierce, S. E., Kitchener, A. C., Goswami, A. and Hutchinson, J. R. (2016). The scaling of postcranial muscles in cats (Felidae) II: hindlimb and lumbosacral muscles. *J. Anat.* **229**, 142-152. doi:10.1111/joa.12474

Daley, M. A. and Birn-Jeffery, A. (2018). Scaling of avian bipedal locomotion reveals independent effects of body mass and leg posture on gait. *J. Exp. Biol.* **221**, jeb152538. doi:10.1242/jeb.152538

Day, L. M. and Jayne, B. C. (2007). Interspecific scaling of the morphology and posture of the limbs during the locomotion of cats (Felidae). *J. Exp. Biol.* **210**, 642-654. doi:10.1242/jeb.02703

Demes, B., Larson, S. G., Stern, J. T., Jungers, W. L., Biknevicius, A. R. and Schmitt, D. (1994). The kinetics of primate quadrupedalism: "hindlimb drive" reconsidered. *J. Hum. Evol.* **26**, 353-374. doi:10.1006/jhev.1994.1023

Dick, T. J. M. and Clemente, C. J. (2017). Where have all the giants gone? How animals deal with the problem of size. *PLoS Biol.* **15**, e2000473. doi:10.1371/journal.pbio.2000473

Dodson, P. (1975). Functional and ecological significance of relative growth in *Alligator*. *J. Zool. Lond.* **175**, 315-355. doi:10.1111/j.1469-7998.1975.tb01405.x

Druelle, F., Aerts, P., D'Août, K., Moulin, V. and Berillon, G. (2017). Segmental morphometrics of the olive baboon (*Papio anubis*): a longitudinal study from birth to adulthood. *J. Anat.* **230**, 805-819. doi:10.1111/joa.12602

Erickson, G. M., Lappin, A. K. and Vliet, K. A. (2003). The ontogeny of bite-force performance in American alligator (*Alligator mississippiensis*). *J. Zool.* **260**, 317-327. doi:10.1017/S0952836903003819

Farlow, J. O. and Britton, A. (2000). Size and body proportions in *Alligator mississippiensis*: implications for archosaurian ichnology. *Paleontol. Soc. Korea Spec. Publ.* **4**, 189-206.

Farlow, J. O., Hurlburt, G. R., Elsey, R. M., Britton, A. R. C. and Langston, W. J. (2005). Femoral dimensions and body size of *Alligator mississippiensis*: estimating the size of extinct mesoeucrocodylians. *J. Vertebr. Paleontol.* **25**, 354-369. doi:10.1671/0272-4634(2005)025[0354:FDABSO]2.0.CO;2

Farlow, J. O., Robinson, N. J., Kumagai, C. J., Paladino, F. V., Falkingham, P. L., Elsey, R. M. and Martin, A. J. (2018). Trackways of the American crocodile (*Crocodylus acutus*) in northwestern Costa Rica: implications for crocodylian ichnology. *Ichnos* **25**, 30-65. doi:10.1080/10420940.2017.1350856

Gatesy, S. M. (1990). Caudefemoral musculature and the evolution of theropod locomotion. *Paleobiology* **16**, 170-186. doi:10.1017/S0094837300009866

Gatesy, S. M. (1991). Hind limb movements of the American alligator (*Alligator mississippiensis*) and postural grades. *J. Zool.* **224**, 577-588. doi:10.1111/j.1469-7998.1991.tb03786.x

Gatesy, S. M. (1997). An electromyographic analysis of hindlimb function in *Alligator* during terrestrial locomotion. *J. Morphol.* **234**, 197-212. doi:10.1002/(SICI)1097-4687(199711)234:2<197::AID-JMOR6>3.0.CO;2-9

Gatesy, S. M. and Biewener, A. A. (1991). Bipedal locomotion: effects of speed, size and limb posture in birds and humans. *J. Zool.* **224**, 127-147. doi:10.1111/j.1469-7998.1991.tb04794.x

Gignac, P. M. and Erickson, G. M. (2016). Ontogenetic bite-force modeling of *Alligator mississippiensis*: implications for dietary transitions in a large-bodied vertebrate and the evolution of crocodylian feeding. *J. Zool.* **299**, 229-238. doi:10.1111/jzo.12349

Granatosky, M. C. (2016). A mechanical analysis of suspensory locomotion in primates and other mammals. *PhD dissertation*, Duke University, Durham.

Granatosky, M. C., Fitzsimons, A., Zeininger, A. and Schmitt, D. (2018). Mechanisms for the functional differentiation of the propulsive and braking roles of the forelimbs and hindlimbs during quadrupedal walking in primates and felines. *J. Exp. Biol.* **221**, 162917. doi:10.1242/jeb.162917

Grand, T. I. (1983). The anatomy of growth and its relation to locomotor capacity in *Macaca*. In *Advances in the Study of Mammalian Behavior* (ed. J. F. Eisenberg and D. G. Kleiman), pp. 5-23. Shippensburg: American Society of Mammalogists.

Gray, J. (1968). *Animal Locomotion*. New York: W. W. Norton & Company.

Gregory, W. K. (1912). Notes on the principles of quadrupedal locomotion and on the mechanism of the limbs in hoofed animals. *Ann. N. Y. Acad. Sci.* **22**, 267-294. doi:10.1111/j.1749-6632.1912.tb55164.x

Grossi, B. and Canals, M. (2010). Comparison of the morphology of the limbs of juvenile and adult horses (*Equus caballus*) and their implications on the locomotor biomechanics. *J. Exp. Zool. A Ecol. Genet. Physiol.* **313A**, 292-300. doi:10.1002/jez.598

Harper, C. M. and Sylvester, A. D. (2019). Effective mechanical advantage allometry of felid elbow and knee extensors. *Anat. Rec.* **302**, 775-784. doi:10.1002/ar.23973

Hedrick, T. L. (2008). Software techniques for two- and three-dimensional kinematic measurements of biological and biomimetic systems. *Bioinspir. Biomim.* **3**, 034001. doi:10.1088/1748-3182/3/3/034001

Heglund, N. C. and Taylor, C. R. (1988). Speed, stride frequency and energy cost per stride: how do they change with body size and gait? *J. Exp. Biol.* **138**, 301-318. doi:10.1242/jeb.138.1.301

Helmsmüller, D., Anders, A., Nolte, I. and Schilling, N. (2014). Ontogenetic change of the weight support pattern in growing dogs. *J. Exp. Zool. A Ecol. Genet. Physiol.* **321**, 254-264. doi:10.1002/jez.1856

Hildebrand, M. (1976). Analysis of tetrapod gaits: general considerations and symmetrical gaits. In *Neural Control of Locomotion* (ed. R. M. Herman, S. Grillner, P. S. G. Stein and D. G. Stuart), pp. 203-236. New York: Plenum Press.

Hothorn, T., Bretz, F. and Westfall, P. (2008). Simultaneous inference in general parametric models. *Biometrical J.* **50**, 346-363. doi:10.1002/bimj.200810425

Howland, D. R., Bregman, B. S. and Goldberger, M. E. (1995). The development of quadrupedal locomotion in the kitten. *Exp. Neurol.* **135**, 93-107. doi:10.1006/exnr.1995.1070

Hudson, P. E., Corr, S. A. and Wilson, A. M. (2012). High speed galloping in the cheetah (*Acinonyx jubatus*) and the racing greyhound (*Canis familiaris*): spatio-temporal and kinetic characteristics. *J. Exp. Biol.* **215**, 2425-2434. doi:10.1242/jeb.066720

Hutchinson, J. R., Felkler, D., Houston, K., Chang, Y.-M., Brueggen, J., Kledzik, D. and Vliet, K. A. (2019). Divergent evolution of terrestrial locomotor abilities in extant Crocodylia. *Sci. Rep.* **9**, 19302. doi:10.1038/s41598-019-55768-6

Iijima, M. and Kubo, T. (2019). Allometric growth of limb and body proportions in crocodylians. *J. Zool.* **309**, 200-211. doi:10.1111/jzo.12714

Iijima, M., Kubo, T. and Kobayashi, Y. (2018). Comparative limb proportions reveal differential locomotor morphofunctions of alligatoroids and crocodyloids. *R. Soc. Open Sci.* **5**, 171774. doi:10.1098/rsos.171774

Irschick, D. J. and Jayne, B. C. (1999). Comparative three-dimensional kinematics of the hindlimb for high-speed bipedal and quadrupedal locomotion of lizards. *J. Exp. Biol.* **202**, 1047-1065. doi:10.1242/jeb.202.9.1047

Irschick, D. J. and Jayne, B. C. (2000). Size matters: ontogenetic variation in the three-dimensional kinematics of steady-speed locomotion in the lizard *Dipsosaurus dorsalis*. *J. Exp. Biol.* **203**, 2133-2148. doi:10.1242/jeb.203.14.2133

Jenkins, F. A. (1971). Limb posture and locomotion in the Virginia opossum (*Didelphis marsupialis*) and in other non–cursorial mammals. *J. Zool.* **165**, 303-315. doi:10.1111/j.1469-7998.1971.tb02189.x

Karakasiliotis, K., Schilling, N., Cabelguen, J.-M. and Ijspeert, A. J. (2013). Where are we in understanding salamander locomotion: biological and robotic perspectives on kinematics. *Biol. Cybern.* **107**, 529-544. doi:10.1007/s00422-012-0540-4

Kawano, S. M., Economy, D. R., Kennedy, M. S., Dean, D. and Blob, R. W. (2016). Comparative limb bone loading in the humerus and femur of the tiger salamander: testing the "mixed-chain" hypothesis for skeletal safety factors. *J. Exp. Biol.* **219**, 341-353. doi:10.1242/jeb.125799

Kimura, T., Okada, M. and Ishida, H. (1979). Kinesiological characteristics of primate walking: its significance in human walking. In *Environment, Behavior and Morphology: Dynamic Interactions in Primates* (ed. M. E. Morbeck, H. Preuschoft and N. Gomberg), pp. 297-311. New York: G. Fischer.

Kram, R. and Taylor, C. R. (1990). Energetics of running: a new perspective. *Nature* **346**, 265-267. doi:10.1038/346265a0

Lüdecke, D., Makowski, D., Waggoner, P. and Patil, I. (2020). Assessment of regression models performance. *CRAN*. doi:10.5281/zenodo.3952174

Manafzadeh, A. R. and Gatesy, S. M. (2021). Paleobiological reconstructions of articular function require all six degrees of freedom. *J. Anat.* **239**, 1516-1524. doi:10.1111/joa.13513

Manafzadeh, A. R., Kambic, R. E. and Gatesy, S. M. (2021). A new role for joint mobility in reconstructing vertebrate locomotor evolution. *Proc. Natl. Acad. Sci. USA* **118**, e2023513118. doi:10.1073/pnas.2023513118

McElroy, E. J., Wilson, R., Biknevicius, A. R. and Reilly, S. M. (2014). A comparative study of single-leg ground reaction forces in running lizards. *J. Exp. Biol.* **217**, 735-742. doi:10.1242/jeb.095620

McMahon, T. (1973). Size and shape in biology. *Science* **179**, 1201-1204. doi:10.1126/science.179.4079.1201

McMahon, T. A. (1975a). Using body size to understand the structural design of animals: quadrupedal locomotion. *J. Appl. Physiol.* **39**, 619-627. doi:10.1152/jappl.1975.39.4.619

McMahon, T. A. (1975b). Allometry and biomechanics: limb bones in adult ungulates. *Am. Nat.* **109**, 547-563. doi:10.1086/283026

McMahon, T. A., Valiant, G. and Frederick, E. C. (1987). Groucho running. *J. Appl. Physiol.* **62**, 2326-2337. doi:10.1152/jappl.1987.62.6.2326

Merkens, H. W., Schamhardt, H. C., Hartman, W. and Kersjes, A. W. (1985). Ground reaction force patterns of Dutch Warmblood horses at normal walk. *Equine Vet. J.* **18**, 207-214. doi:10.1111/j.2042-3306.1986.tb03600.x

Moisio, K. C., Sumner, D. R., Shott, S. and Hurwitz, D. E. (2003). Normalization of joint moments during gait: a comparison of two techniques. *J. Biomech.* **36**, 599-603. doi:10.1016/S0021-9290(02)00433-5

Nesbitt, S. J. (2011). The early evolution of archosaurs: relationships and the origin of major clades. *Bull. Am. Museum Nat. Hist.* **352**, 1-292. doi:10.1206/352.1

Nyakatura, J. A., Andrada, E., Curth, S. and Fischer, M. S. (2014). Bridging "Romer's gap": limb mechanics of an extant belly-dragging lizard inform debate on tetrapod locomotion during the Early Carboniferous. *Evol. Biol.* **41**, 175-190. doi:10.1007/s11692-013-9266-z

Nyakatura, J. A., Melo, K., Horvat, T., Karakasiliotis, K., Allen, V. R., Andikfar, A., Andrada, E., Arnold, P., Lauströer, J., Hutchinson, J. R. et al. (2019). Reverse-engineering the locomotion of a stem amniote. *Nature* **565**, 351-355. doi:10.1038/s41586-018-0851-2

Parrish, J. M. (1986). Locomotor adaptations in the hindlimb and pelvis of the Thecodontia. *Hunteria* **1**, 1-35.

Parrish, J. M. (1987). The origin of crocodilian locomotion. *Paleobiology* **13**, 396-414. doi:10.1017/S0094837300009003

Patel, B. A., Horner, A. M., Thompson, N. E., Barrett, L., Henzi, S. P. (2013). Ontogenetic scaling of fore- and hind limb posture in wild Chacma baboons (*Papio hamadryas ursinus*). *PLoS ONE* **8**, e71020. doi:10.1371/journal.pone.0071020

Peters, S. E. (1983). Postnatal development of gait behaviour and functional allometry in the domestic cat (*Felis catus*). *J. Zool.* **199**, 461-486. doi:10.1111/j.1469-7998.1983.tb05100.x

Polk, J. D. (2002). Adaptive and phylogenetic influences on musculoskeletal design in cercopithecine primates. *J. Exp. Biol.* **205**, 3399-3412. doi:10.1242/jeb.205.21.3399

Pollock, C. M. and Shadwick, R. E. (1994). Allometry of muscle, tendon, and elastic energy storage capacity in mammals. *Am. J. Physiol.* **266**, R1022-R1031. doi:10.1152/ajpregu.1994.266.3.R1022

Reilly, S. M. and Blob, R. W. (2003). Motor control of locomotor hindlimb posture in the American alligator (*Alligator mississippiensis*). *J. Exp. Biol.* **206**, 4327-4340. doi:10.1242/jeb.00688

Reilly, S. M. and Elias, J. A. (1998). Locomotion in *Alligator mississippiensis*: kinematic effects of speed and posture and their relevance to the sprawling-to-erect paradigm. *J. Exp. Biol.* **201**, 2559-2574. doi:10.1242/jeb.201.18.2559

Reilly, S. M., Willey, J. S., Biknevicius, A. R. and Blob, R. W. (2005). Hindlimb function in the alligator: integrating movements, motor patterns, ground reaction forces and bone strain of terrestrial locomotion. *J. Exp. Biol.* **208**, 993-1009. doi:10.1242/jeb.01473

Reilly, S. M., McElroy, E. J. and Biknevicius, A. R. (2007). Posture, gait and the ecological relevance of locomotor costs and energy-saving mechanisms in tetrapods. *Zoology* **110**, 271-289. doi:10.1016/j.zool.2007.01.003

Ren, L., Miller, C. E., Lair, R. and Hutchinson, J. R. (2010). Integration of biomechanical compliance, leverage, and power in elephant limbs. *Proc. Natl. Acad. Sci. USA* **107**, 7078-7082. doi:10.1073/pnas.0911396107

Schmitt, D. (1999). Compliant walking in primates. *J. Zool.* **248**, 149-160. doi:10.1111/j.1469-7998.1999.tb01191.x

Schmitt, D. and Hanna, J. B. (2004). Substrate alters forelimb to hindlimb peak force ratios in primates. *J. Hum. Evol.* **46**, 237-252. doi:10.1016/j.jhevol.2003.11.008

Self Davies, Z. T., Spence, A. J. and Wilson, A. M. (2019). Ground reaction forces of overground galloping in ridden Thoroughbred racehorses. *J. Exp. Biol.* **222**, 204107. doi:10.1242/jeb.204107

Shine, C. L., Penberthy, S., Robbins, C. T., Nelson, O. L. and McGowan, C. P. (2015). Grizzly bear (*Ursus arctos horribilis*) locomotion: gaits and ground reaction forces. *J. Exp. Biol.* **218**, 3102-3109. doi:10.1242/jeb.121806

Singh, L. A. K. and Bustard, H. R. (1976). Locomotory behaviour during basking and spoor formation in the gharial (*Gavialis gangeticus*). *Br. J. Herpetol.* **5**, 673-676.

Sullivan, C. S. (2007). Function and evolution of the hind limb in Triassic archosaurian reptiles. *PhD dissertation*, Harvard University, Cambridge, MA.

Turnquist, J. E. and Wells, J. P. (1994). Ontogeny of locomotion in rhesus macaques (*Macaca mulatta*): I. Early postnatal ontogeny of the musculoskeletal system. *J. Hum. Evol.* **26**, 487-499. doi:10.1006/jhev.1994.1029

Vilensky, J. A. and Gankiewicz, E. (1989). Early development of locomotor behavior in vervet monkeys. *Am. J. Primatol.* **17**, 11-25. doi:10.1002/ajp.1350170103

Willey, J. S., Biknevicius, A. R., Reilly, S. M. and Earls, K. D. (2004). The tale of the tail: limb function and locomotor mechanics in *Alligator mississippiensis*. *J. Exp. Biol.* **207**, 553-563. doi:10.1242/jeb.00774

Wiseman, A. L. A., Bishop, P. J., Demuth, O. E., Cuff, A. R., Michel, K. B. and Hutchinson, J. R. (2021). Musculoskeletal modelling of the Nile crocodile (*Crocodylus niloticus*) hindlimb: effects of limb posture on leverage during terrestrial locomotion. *J. Anat.* **239**, 424-444. doi:10.1111/joa.13431

Xu, R. (2003). Measuring explained variation in linear mixed effects models. *Stat. Med.* **22**, 3527-3541. doi:10.1002/sim.1572

Young, J. W. (2009). Ontogeny of joint mechanics in squirrel monkeys (*Saimiri boliviensis*): functional implications for mammalian limb growth and locomotor development. *J. Exp. Biol.* **212**, 1576-1591. doi:10.1242/jeb.025460

Young, J. W. (2012). Ontogeny of limb force distribution in squirrel monkeys (*Saimiri boliviensis*): insights into the mechanical bases of primate hind limb dominance. *J. Hum. Evol.* **62**, 473-485. doi:10.1016/j.jhevol.2012.01.003

Young, J. W. and Shapiro, L. J. (2018). Developments in development: what have we learned from primate locomotor ontogeny? *Am. J. Phys. Anthropol.* **165**, 37-71. doi:10.1002/ajpa.23388

Zeininger, A., Shapiro, L. J. and Raichlen, D. A. (2017). Ontogenetic changes in limb postures and their impact on effective limb length in baboons (*Papio cynocephalus*). *Am. J. Phys. Anthropol.* **163**, 231-241. doi:10.1002/ajpa.23201

Zumwalt, A. C., Hamrick, M. and Schmitt, D. (2006). Force plate for measuring the ground reaction forces in small animal locomotion. *J. Biomech.* **39**, 2877-2881. doi:10.1016/j.jbiomech.2005.10.006